Comparative Proteomic Analysis of Histone Post-translational Modifications upon Ischemia/Reperfusion-Induced Retinal Injury

ARTICLE *in* JOURNAL OF PROTEOME RESEARCH · MARCH 2014

Impact Factor: 4.25 · DOI: 10.1021/pr500040a · Source: PubMed

7 AUTHORS, INCLUDING:

Simone Sidoli
University of Pennsylvania
30 PUBLICATIONS **182** CITATIONS
SEE PROFILE

Leilei Wang
University of Texas Southwestern Medical Cen…
8 PUBLICATIONS **102** CITATIONS
SEE PROFILE

Ole N Jensen
University of Southern Denmark
296 PUBLICATIONS **18,804** CITATIONS
SEE PROFILE

Ling Zheng
Wuhan University
47 PUBLICATIONS **1,466** CITATIONS
SEE PROFILE

Journal of proteome research

Article

pubs.acs.org/jpr

Comparative Proteomic Analysis of Histone Post-translational Modifications upon Ischemia/Reperfusion-Induced Retinal Injury

Xiaolu Zhao,[†] Simone Sidoli,[‡] Leilei Wang,[†] Wenjun Wang,[†] Lin Guo,*[,†] Ole N. Jensen,*[,‡] and Ling Zheng*[,†]

[†]College of Life Sciences, Wuhan University, Wuhan 430072, P. R. China

[‡]Department of Biochemistry and Molecular Biology, University of Southern Denmark, DK-5230 Odense M, Denmark

Supporting Information

ABSTRACT: We present a detailed quantitative map of single and coexisting histone post-translational modifications (PTMs) in rat retinas affected by ischemia and reperfusion (I/R) injury. Retinal I/R injury contributes to serious ocular diseases, which can lead to vision loss and blindness. We applied linear ion trap−orbitrap hybrid tandem mass spectrometry (MS/MS) to quantify 131 single histone marks and 143 combinations of multiple histone marks in noninjured and injured retinas. We observed 34 histone PTMs that exhibited significantly ($p < 0.05$) different abundance between healthy and I/R injured eyes, of which we confirmed three H4 histone marks by Western blotting. H4K20me2 was up to 4-fold change up-regulated after the injury and is associated with the response to DNA damage as demonstrated by an increase in the phosphorylation of p53 and Chk1. This study demonstrates that quantitative MS provides a sensitive and accurate way to dissect the changes in the histone code after retinal injury. Specifically, DNA damage associated histone PTMs may contribute to neurovascular degeneration during the process of ischemia/reperfusion injury.

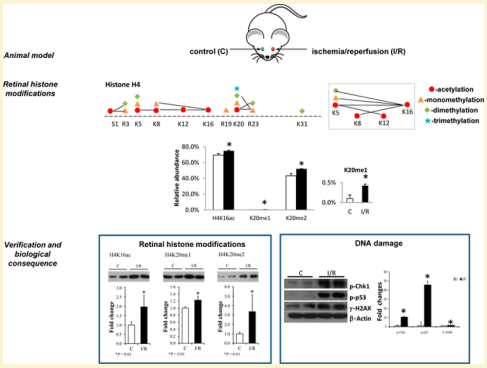

KEYWORDS: *retina, ischemia/reperfusion injury, histones, PTMs, LC−MS/MS, label-free quantitation, DNA damage*

INTRODUCTION

Retinal ischemia contributes to numerous ocular diseases, including glaucoma and diabetic retinopathy, and leads to visual impairment and blindness in patients.[1,2] Rodent model of acute ischemia caused by elevated intraocular pressure followed by reperfusion (I/R) has been used to investigate the molecular mechanisms and to identify potential therapeutic strategies for retinal ischemic injury.[3−5] Previous proteomic studies have demonstrated that there are more than 70 proteins altered after retinal I/R injury in rats, including histone H4,[6,7] suggesting alterations in histones or histone post-translational modifications (PTMs) may contribute to the I/R injury-induced neurovascular degeneration.

Histones can be heavily decorated with numerous PTMs, such as acetylation, methylation, and phosphorylation at distinct amino acid residues.[8] Histone modifications have important functions related to regulation of gene transcription, cell cycle, apoptosis, cell fate determination, etc.[9−12] Dysregulation or unbalanced levels of histone modifications are associated with different human diseases, including cancer, neurodegenerative diseases, and inflammation.[13−15] Recent studies have revealed that histone PTMs are rearranged during the development of retina in rodents,[16−19] confirming that histone modifications are crucial in determining cell phenotype. Taken together, an in-depth characterization of histone PTMs in retinal I/R injury would provide valuable information for elucidating the pathogenesis of several retinal diseases.

Mass spectrometry (MS) based proteomics has become an integrated and indispensable tool in modern chromatin biology, providing insights into the mechanisms and dynamics of epigenetic processes. Due to the high sensitivity, high mass accuracy, precise peptide sequencing, and the possibility to perform large-scale analyses, this technique is highly suitable for characterizing PTMs on histones. A range of analytical methods and MS-based strategies for histone analysis are available, among which the bottom-up strategy is the most widely used for protein characterization at present.[20] Analysis of peptides of 7−20 amino acids allows not only the quantification of single PTMs, but also coexisting ones. This permits the characterization of PTM cross-talk, which is crucial for in-depth understanding of the role of histone marks in fine-tuning gene regulation and development.

In the present study, we performed a quantitative proteomic study on rat retina to investigate the changes of histone PTMs after I/R injury. We report profiles of individual and coexisting histone PTMs after retinal injury. Based on liquid chromatography (LC) and collision-induced dissociation (CID) MS/MS, we generated a data set containing a total of 236 distinct

Received: January 13, 2014
Published: March 14, 2014

   dx.doi.org/10.1021/pr500040a | J. Proteome Res. 2014, 13, 2175−2186

peptides from H1, H2A, H2B, H3, and H4 and their variants in the rat retina. One hundred forty-three of these peptides carried between one and seven PTMs, resulting in 131 unique PTMs. A total of seven PTMs in H3, six PTMs in H4, and 21 PTMs in other histone proteins (H2A, H2B, H1, and their variants) were found to have significantly ($p < 0.05$) different abundance after I/R injury. Some of these histone marks were further verified by Western blotting using commercially available antibodies, including H4K20me1 and H4K20me2. Upregulation of these two histone marks is related to DNA damage.[21−23]

EXPERIMENTAL PROCEDURES

Materials

Pure water was obtained from a Milli-Q system (Millipore, Bedford, MA). ArgC was from G-Biosciences (USA). Poros Oligo R3 reversed-phase material was from PerSeptive Biosystems (Framingham, MA). All other reagents and solvents were of the highest commercial quality and were used without further purification.

Rat Model of Retinal I/R

Male Wistar rats (160−180 g) were obtained from the Hubei Animal Laboratory and housed in ventilated microisolator cages with free access to water and food. Retinal I/R injury was induced as previously described.[16,24] The duration of ischemia was 60 min. Retinas were collected at 2 days after I/R injury. All procedures involving the animals were approved by the Committee on Ethics in the Care and Use of Laboratory Animals of College of Life Sciences at Wuhan University.

Histone Extraction and 2D Analysis

Histones were extracted as previously described.[16] Freshly isolated retinas were homogenized in hypotonic lysis buffer with phos-STOP (Roche, Basel, Switzerland) and Protease Inhibitor Cocktail (Roche). The samples were further lysed by hypotonic lysis buffer with 10% NP-40 for 10 min on ice. The nuclei were collected and histones were extracted by incubated the nuclei with 0.2 M H_2SO_4. Histones were then reprecipitated by 100% trichloroacetic acid (TCA). After being washed with acetone, histones were dissolved in dH_2O, and the concentration was quantitated using the Bio-Rad Protein Assay (Bio-Rad, Hercules, CA).

Histones (20 μg) were used for 2D analysis (triton acid urea (TAU)/acid urea (AU)-SDS PAGE) as previously described.[25] Briefly, a short 15% TAU gel or AU gel was used for first-dimensional electrophoresis followed by a 15% SDS PAGE as the second-dimensional electrophoresis. After electrophoresis, the gels were stained by Deep Purple Total Protein Stain (GE Healthcare, Germany) and scanned with a laser scanner (Typhoon 9200, Amersham, Sweden).

Western Blots

Freshly isolated retinas were sonicated in ice-cold RIPA buffer (Beyotime, China) as previously reported.[26] Extracted histones (0.5 μg) or 20 μg of whole retinal lysates were separated by SDS-PAGE and electroblotted onto PVDF membrane (Millipore, Billerica, MA). Antibodies for H3K9ac (1:5000), H4K8ac (1:2000), H4K12ac (1:5000), phosphorylated-p53-(Ser15) (1:1000), phosphorylated-Chk1(Ser345) (1:1000), and γ-H2AX (also called phosphorylated-H2AX(Ser139)) (1:1000) were obtained from Cell Signaling Technology (Beverly, MA); antibodies for H3K9me2 (1:5000), H3K9me3 (1:10000), and β-actin (1:10000) were obtained from Abcam (Cambridge, England); antibodies for H3K27me1 (1:5000), H3K27me2 (1:5000), and H3K79me2 (1:5000) were obtained from Millipore (Billerica, MA); antibodies for H3K79me1 (1:5000), H4K16ac (1:5000), H4K20me1 (1:5000), H4K20me2 (1:5000), and H4K20me3 (1:5000) were obtained from Active Motif (Carlsbad, CA); antibody for p53 (1:500) was obtained from Santa Cruz Biotechnology (Santa Cruz, CA). Protein bands detected by the antibodies were visualized by enhanced chemiluminescence (ECL, Perice, IL) and evaluated by the Quantity One 1-D Analysis Software (Bio-Rad). The levels of modified histones were first quantitated relative to the Coomassie staining in the same sample, levels of other target proteins were first quantitated relative to β-actin in the same sample, and then the relative expression levels in different group were normalized to control groups which set up as 1-fold.

Protein Digestion

After histone precipitation by TCA, the pellet was resuspended in 100 mM NH_4HCO_3, 1 mM calcium acetate, and 7.5 mM DTT. ArgC digestion enzyme was added to 20 μg of sample with an enzyme/sample ratio of 1:50, and the sample was digested overnight at 37°. Digestion was interrupted by addition of 1% TFA to the solution.

Mass Spectrometry of Histone Peptides

Samples were loaded and separated with an EASY-nLC nanoHPLC (Proxeon, Odense, Denmark) using a two-column setup; the setup consisted of a 100 μm i.d. × 2 cm Reprosil-Pur C18-AQ (3 μm; Dr. Maisch GmbH, Germany) trap column and a 75 μm i.d. × 17 cm Reprosil-Pur C18-AQ (3 μm; Dr. Maisch GmbH) nanocolumn. Injection volume was set to 5 μL. The HPLC gradient was 0−34% solvent B (A = 0.1% formic acid; B = 95% MeCN, 0.1% formic acid) over 60 min and from 34% to 100% solvent B in 5 min at a flow-rate of 250 nL/min. Liquid chromatography (LC) was coupled with an LTQ-Orbitrap XL mass spectrometer (ThermoFisher Scientific, Bremen, Germany).

Nanoelectrospray (Proxeon) was used with a spray voltage of 2.3 kV. No sheath, sweep, and auxiliary gases were used, and capillary temperature was set to 200 °C. The LTQ-Orbitrap XL instrument was used in data-dependent MS/MS acquisition mode. Acquisition was performed in the Orbitrap for MS with a resolution of 60000 (full-width at half-height) and in the linear ion trap (LTQ) for MS/MS. Maximum injection time was set at 1 s for MS and 100 ms for MS/MS. The MS m/z acquisition window was set at 300−1650. Precursor charge states 1+ and unassigned were excluded. The 10 most intense ions over a threshold of 5,000 counts were isolated for fragmentation in the LTQ using CID, with an activation Q value of 0.25 and activation time of 15 ms. The dynamic exclusion time was set to 60 s.

Data Processing and Database Search

Data were processed using Proteome Discoverer v1.3.0.339 (Thermo Scientific). Mascot v2.3 (Matrix Science) was used for database search. A list of rat and mouse histones was downloaded from Uniprot (updated at 5/09/2011). ArgC was selected as digestion enzyme, and two missed cleavages were allowed. MS mass tolerance was set to 8 ppm, while MS/MS tolerance was set to 0.6 Da. No fixed modifications were allowed, while dynamic modifications included were acetylation (protein N-term and K), methylation (KR), dimethylation (KR), and trimethylation (K). Peptide validation was performed using the Fixed Value Peptide validator, which

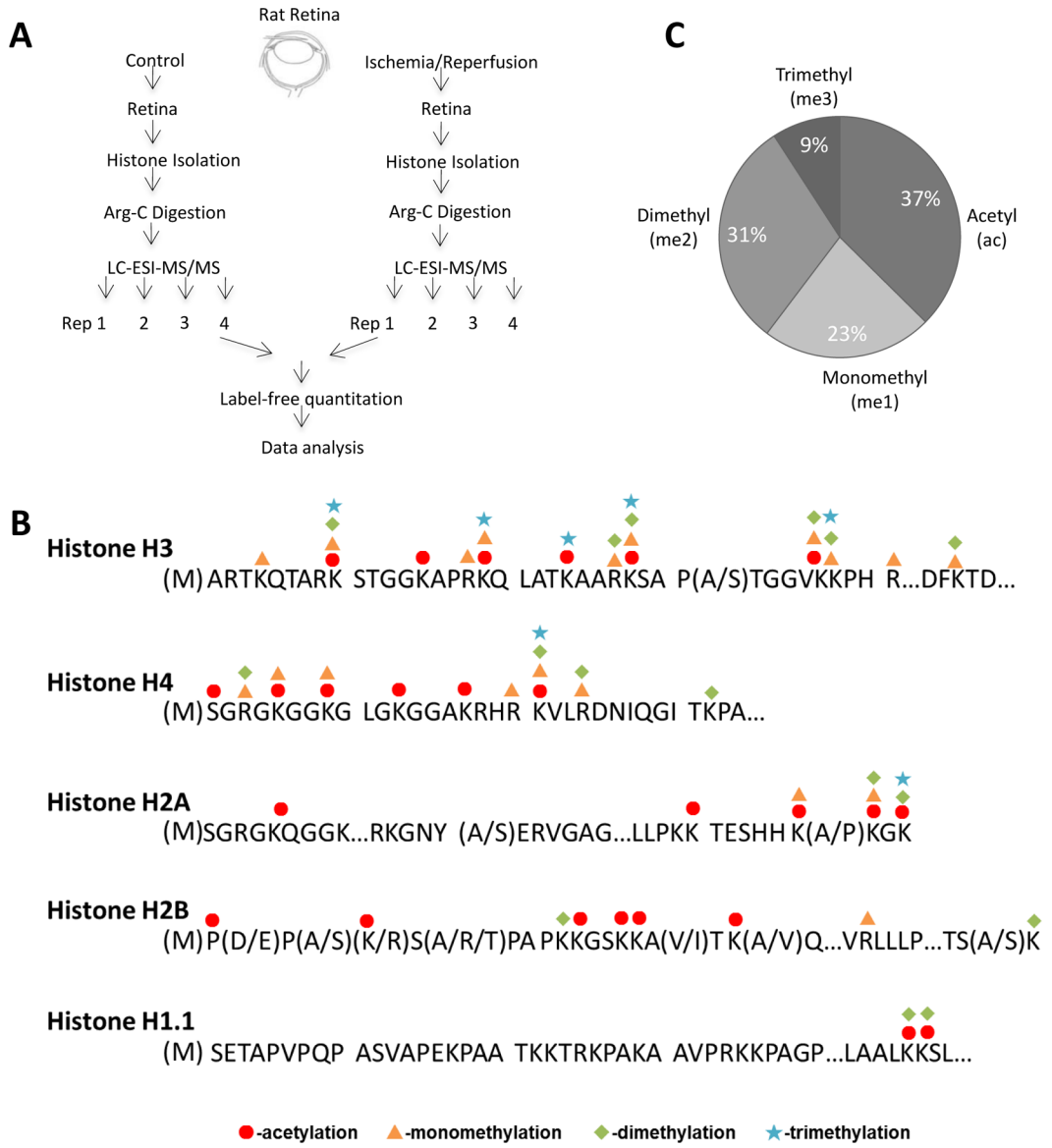

Figure 1. (A) workflow. Samples were prepared in parallel by using the left and the right eye of the rat, corresponding to control and I/R injured, respectively. (B) Position and type of PTMs identified in rat retina in the present study. (C) Relative abundance of the quantified PTMs on all detected histones.

uses a fixed score threshold to estimate peptide confidence without performing decoy database searching. The quality of MS/MS spectra was manually evaluated to ensure the threshold was set correctly. Peptides were filtered with the following parameters: mascot score >20, peptide rank = 1, and peptide confidence 5%. Quantification was performed using Progenesis LC-MS v4.0 (Nonlinear dynamics) using default settings for peak area extraction. Each quantified peptide was divided by the quantification of the respective peptide in all the modified states (including unmodified form) in order to obtain an estimation of the modified sites in percentage of the total signal obtained for a particular histone species. We manually verified the quantification of coexisting marks whether they were identified in a peptide with a missed cleavage in between the two or more PTMs. In case we also identified the sequence without missed cleavages such a coexisting mark was discarded, as it was not possible to calculate the relative abundance of such PTM combinations when truncated in between by proteolytic cleavage.

Statistical Analysis

All quantitative results were expressed as the mean ± SEM. For two-group comparison, data was analyzed by the *t* test with equal variance. Differences were considered statistically significant when the P values were less than 0.05.

RESULTS AND DISCUSSION

Retinal I/R Induced Alteration in Histones and Possible Histone PTMs Exhibited by 2D Electrophoresis

Extracted histones from I/R-injured and noninjured retinas were separated by either TAU-SDS PAGE (to separate histone PTMs and variants) or AU-SDS PAGE (to separate histone PTMs).[25] As shown in Supplemental Figure 1 (Supporting Information), I/R-induced histones changed in spot size and tailing in at least five different places, indicating alteration of certain histone variants and histone PTMs after the injury. MS analysis identified several histones and variants in these spots (Supplemental Figure 1, Supporting Information). However,

dx.doi.org/10.1021/pr500040a | J. Proteome Res. 2014, 13, 2175−2186

Table 1. Quantified H3 Peptides[a]

protein	peptide/site	modification	control (%)	I/R (%)	ratio	*P* value
H3	$TK_4QTARKSTGGKAPR$	K4me1	100 ± 0	100 ± 0	1.0	
	$K_9STGGK_{14}APR_{17}$	unmodified	0.01 ± 0.01	0.039 ± 0.002	0.3	0.271
		K9ac	1.7 ± 1.48	1.03 ± 0.55	0.6	0.686
		K9me1	20.33 ± 4.44	19.1 ± 2.43	0.9	0.816
		K9me2	14.69 ± 4.19	8.38 ± 3.59	0.6	0.296
		K9me3	4.12 ± 2.17	3.14 ± 1.72	0.8	0.735
		K9acK14ac	6.91 ± 2.74	6.12 ± 0.8	0.9	0.791
		K9me1K14ac	5.36 ± 3.09	6.63 ± 1.19	1.2	0.714
		K9me2K14ac	11.44 ± 10.11	22.12 ± 12.29	1.9	0.527
		K9me3K14ac	11.16 ± 5.33	17.48 ± 6.27	1.6	0.472
		K14ac	21.29 ± 8.17	14.77 ± 8.37	0.7	0.597
		K14acR17me1*	2.98 ± 0.6	1.24 ± 0.16	0.4	0.030
	$K_{18}QLATK_{23}AAR_{26}$	unmodified	24.36 ± 9.32	11.34 ± 5.6	0.5	0.276
		K18ac*	0.32 ± 0.04	0.17 ± 0.02	0.5	0.011
		K18me1	1.44 ± 0.62	0.22 ± 0.02	0.2	0.099
		K18me3	2.63 ± 0.49	2.57 ± 0.19	1.0	0.911
		K18acK23ac	24.01 ± 5.33	21.93 ± 2.33	0.9	0.733
		K18me1K23ac	0.85 ± 0.16	1 ± 0.11	1.2	0.471
		K23ac*	45.2 ± 5.68	61.92 ± 3.1	1.4	0.041
		K23me3	0.06 ± 0.01	0.1 ± 0.03	1.5	0.401
		K23acR26me1*	0.39 ± 0.05	0.24 ± 0.02	0.6	0.041
		R26me2	0.73 ± 0.09	0.51 ± 0.04	0.7	0.069
	$K_{27}SAPATGGVK_{36}K_{37}PHR_{40}$	unmodified	0.31 ± 0.04	0.2 ± 0.02	0.6	0.026
		K27me1	3.65 ± 0.56	2.76 ± 0.09	0.8	0.172
		K27me1K36me2	13.38 ± 0.7	13.37 ± 1.09	1.0	0.995
		K27me2*	18.61 ± 0.43	13.81 ± 0.55	0.7	0.000
		K27me2K36acK37me3R40me1§	0.39 ± 0.07	0.3 ± 0.02	0.8	0.231
		K27me2K36me1*	0.3 ± 0.04	0.15 ± 0.02	0.5	0.020
		K27me2K36me2*	61.01 ± 1.63	67.24 ± 1.84	1.1	0.045
		K27me3K36me2	1.79 ± 0.13	1.82 ± 0.21	1.0	0.885
		K36acK37me3*§	0.56 ± 0.05	0.33 ± 0.03	0.6	0.009
	$EIAQDFK_{79}TDLR$	unmodified	78.44 ± 0.59	77.27 ± 0.31	1.0	0.130
		K79me1	18.71 ± 0.38	19.48 ± 0.21	1.0	0.122
		K79me2	2.85 ± 0.24	3.25 ± 0.12	1.1	0.198
H3.3	$K_{27}SAPSTGGVK_{36}K_{37}PHR_{40}$	unmodified	0.73 ± 0.15	0.2 ± 0.07	0.3	0.017
		K27ac	0.08 ± 0.01	0.08 ± 0.004	1.1	0.511
		K27me2	39.23 ± 2.81	30.55 ± 3.15	0.8	0.086
		K27acK37me1*	0.08 ± 0.004	0.06 ± 0.002	0.8	0.007
		K27acK37me2	0.62 ± 0.03	0.49 ± 0.04	0.8	0.053
		K27acK37me2R40me1	0.12 ± 0.01	0.12 ± 0.01	1.0	0.962
		K27me1K36me2	32.35 ± 1.52	39.22 ± 3	1.2	0.087
		K27me2K36me2	26.81 ± 2.43	29.27 ± 4.97	1.1	0.671

[a]Those which were significantly altered after I/R injury are marked with an asterisk. The MS analysis we adopted could not discriminate between the two forms H3K36acK37me3 and H3K36me3K37ac. This co-existing PTM is to be considered as ambiguous (marked with §).

this preliminary analysis did not characterize which histone modifications are affected by retinal I/R injury.

Profiling Histone PTMs in Retinas after I/R Injury by MS Analysis

A quantitative proteomics analysis was performed on the extracted histones from the retinas with or without I/R injury. The schematic workflow of this proteomic survey is shown in Figure 1A. Retinal ischemia was induced as previously reported,[3,4] and histones were extracted as described in the Experimental Procedures. Histones were digested using ArgC, which cleaved at the C-terminal of arginine residues, to generate peptides with proper size (7−20 aa). The digested histone peptides were analyzed in four technical replicates by nanoLC-ESI-MS/MS analysis. The histone PTMs in retinas from the I/R condition, as quantified by MS, were compared with that of the contralateral control eyes. Histone PTMs were quantified relatively to the total amount of the respective peptide sequence. Such normalization was performed to compensate for imprecisions regarding the amount of sample injected. However, the percentage of occupancy of a PTM should be used to estimate its real abundance on the chromatin with a certain degree of inaccuracy, as the ionization efficiency of differently modified peptides might vary depending on the PTMs covalently bound.[27] Because of this, in our work we mainly focused on comparing the two conditions rather than relating the abundances of two PTMs within the same sample.

We demonstrate that quantification of the identified peptides was highly reproducible and up to almost 4 orders of magnitude, as shown by the correlation values between replicates (Supplemental Figure 2, Supporting Information)

dx.doi.org/10.1021/pr500040a | J. Proteome Res. 2014, 13, 2175−2186

Table 2. Quantified H4 Peptides[a]

protein	peptide/site	modification	control	I/R	ratio	*P* value
H4	$GK_5GGK_8GLGK_{12}GGAK_{16}R$	unmodified	5.02 ± 1.9	1.93 ± 1.05	0.4	0.203
		K5ac	0.05 ± 0.04	0.04 ± 0.02	0.9	0.922
		K5me1	0.99 ± 0.42	0.69 ± 0.16	0.7	0.522
		K5acK8ac	0.95 ± 0.13	0.84 ± 0.05	0.9	0.429
		K5acK8acK16ac	11.48 ± 1.32	11.36 ± 0.5	1.0	0.938
		K5acK8acK12acK16ac	9.11 ± 1.29	8.7 ± 0.61	1.0	0.781
		K5acK12acK16ac	7.84 ± 0.88	7.64 ± 0.64	1.0	0.864
		K5acK16ac*	10.71 ± 0.19	12.63 ± 0.38	1.2	0.004
		K5me1K16ac	3.7 ± 1.08	3.32 ± 0.24	0.9	0.739
		K5me2K16ac	0.89 ± 0.16	1 ± 0.19	1.1	0.666
		K8ac	0.07 ± 0.03	0.09 ± 0.05	1.2	0.817
		K8acK12ac	19.71 ± 1.76	21.04 ± 1.5	1.1	0.585
		K8acK12acK16ac	5.47 ± 0.41	4.87 ± 0.33	0.9	0.303
		K8acK16ac	2.86 ± 0.75	2.09 ± 0.24	0.7	0.368
		K8me1K16ac	0.5 ± 0.11	0.58 ± 0.12	1.1	0.669
		K12ac	3.78 ± 3	0.65 ± 0.33	0.2	0.339
		K12acK16ac	4.27 ± 0.81	4.82 ± 0.76	1.1	0.639
		K16ac	12.61 ± 3.09	17.73 ± 1.64	1.4	0.194
		S1ac	25.13 ± 3.12	24.99 ± 0.32	1.0	0.964
		S1acR3me1	63.93 ± 2.66	64.88 ± 0.89	1.0	0.746
		S1acR3me2	10.94 ± 1.29	10.13 ± 0.97	0.9	0.636
	$K_{20}VLR_{23}DNIQGITKPAIR$	unmodified	0.02 ± 0.01	0.03 ± 0.003	1.9	0.099
		K20ac*	0.01 ± 0.004	0.13 ± 0.02	10.4	0.001
		K20me1*	0.1 ± 0.09	0.42 ± 0.04	4.2	0.016
		K20me2*	43.24 ± 2.91	51.9 ± 0.37	1.2	0.026
		K20me3	7.58 ± 0.97	5.64 ± 0.5	0.7	0.125
		K20acR23me1*	0.07 ± 0.01	0.17 ± 0.01	2.5	0.002
		K20acR23me2*	0.01 ± 0.002	0.02 ± 0.001	3.2	0.000
		K20me2R23me1*	7.2 ± 1.27	2.76 ± 0.05	0.4	0.013
		R23me1*	5.16 ± 0.86	2.12 ± 0.04	0.4	0.012
		R23me2	36.61 ± 0.34	36.81 ± 0.33	1.0	0.690
	$HR_{19}KVLRDNIQGITKPAIR$	R19me1	100 ± 0	100 ± 0	1.0	

[a]Those which were significantly altered after I/R injury are marked with an asterisk.

and chromatographic peak area integration (Supplemental Figure 3, Supporting Information). A total of 236 peptides derived from histones H3, H4, H2A, H2B, and H1 and noncanonical variants were quantified by label-free MS using Progenesis LC software. One hundred forty-three of the 236 identified peptides possessed between one and seven PTMs. The number of distinct PTMs identified was 131, distributed as follows: 27 on histone H3, 17 on H4, 34 on H2A, 16 on H2B, and 37 on H1, respectively (main histones as shown in Figure 1B; PTMs information for all histones and their variants was included in Tables 1−3 and Supplemental Tables 1−6, Supporting Information). The PTMs detected were acetylation and methylations (mono-, di-, and trimethylation), particularly on N- and C-terminal regions of the histone sequence. In general, acetylated lysine residues were the most frequent (37%) followed by dimethylated (31%), monomethylated (23%), and trimethylated (9%) (Figure 1C). Of the 131 specific histone marks characterized in the present study, 34 of them (including 7 in H3, 6 in H4, 13 in H2A, 1 in H2B, and 7 in H1) were significantly altered in the I/R injured retinas when compared to that in their contralateral noninjured controls (Table 3 and Supplemental Table 4, Supporting Information). By using the bottom-up MS strategy we generated peptides containing numerous PTM sites; this allowed the characterization not only of single marks, but also coexisting ones. We characterized various patterns of histone PTMs residing on the same peptides, generating detailed information of 143 specific coexisting modification states. Tables 1 and 2 and Supplemental Tables 1−3 (Supporting Information) show an overview of all the coexisting PTMs observed on H3, H4, H2A, H2B and H1 from retinas with or without I/R injury, respectively. Of the 143 combinations of histone modifications characterized in rat retinas, 27 of them (including 9 in H3, 9 in H4, 5 in H2A, 1 in H2B and 3 in H1) were significantly different after I/R injury (Tables 1-2 and Supplemental Tables 1−3, Supporting Information). These findings allowed us to evaluate the possible role of coexisting histone PTMs and their cross-talk during the development of retinal diseases, especially those related to I/R injury.

Single and Coexisting Patterns of PTMs on Histones

Recent studies have shown that PTMs co-occur in specific combinations and patterns to form specific histone codes. These coexisting marks can affect the relative abundance of each other, usually caused by steric hindrance or by enhancing/impeding the binding of histone modifying enzymes,[28] generating a "cross-talk".[28−30] The length of the peptides we generate by ArgC digestion (7−20 aa) does not allow comprehensive overview of the entire protein sequence and its modified state. However, the synergic effect between PTMs on the same histone tail has been mainly observed for nearby modifications; e.g. H3R2meK4me, H3K9me3S10ph, H3S10phK14ac, H3R17meK27ac, and H3K27meK36me.[31,32]

dx.doi.org/10.1021/pr500040a | J. Proteome Res. 2014, 13, 2175−2186

Table 3. Summary of the Regulated and Unregulated PTMs on Histones H3 and H4[a]

regulation	protein	modification	control	I/R	ratio	*P* value
regulated	H3	R17me1*	2.98 ± 0.6	1.24 ± 0.16	0.4	0.03
		R26me1*	0.39 ± 0.05	0.24 ± 0.02	0.6	0.04
		K36ac*§	0.96 ± 0.11	0.63 ± 0.04	0.7	0.03
		K36me1*	0.3 ± 0.04	0.15 ± 0.02	0.5	0.02
		K37me1*	0.08 ± 0.004	0.06 ± 0.002	0.8	0.01
		K37me3*§	0.96 ± 0.11	0.63 ± 0.04	0.7	0.03
		K36me2*	135.33 ± 2.42	150.93 ± 3.22	1.1	0.01
	H4	R23me1*	12.42 ± 2.11	5.05 ± 0.04	0.4	0.01
		K16ac*#	69.43 ± 1.93	74.74 ± 0.97	1.1	0.05
		K20ac*	0.09 ± 0.02	0.32 ± 0.01	3.7	0.00
		K20me1*#	0.1 ± 0.09	0.42 ± 0.04	4.2	0.02
		K20me2*#	50.44 ± 1.66	54.66 ± 0.41	1.1	0.05
		K31me2*	0.01 ± 0.004	0.11 ± 0.02	10.1	0.00
unregulated	H3	K9ac#	8.61 ± 2.41	7.15 ± 1.26	0.8	0.61
		K9me1	25.69 ± 3.82	25.74 ± 3.37	1.0	0.99
		K9me2#	26.13 ± 8.3	30.49 ± 8.71	1.2	0.73
		K9me3#	15.28 ± 4.94	20.61 ± 4.61	1.3	0.46
		K14ac	59.15 ± 7.29	68.35 ± 8.06	1.2	0.43
		K18ac	24.33 ± 5.31	22.1 ± 2.35	0.9	0.71
		K18me1	2.3 ± 0.54	1.23 ± 0.12	0.5	0.10
		K18me3	2.63 ± 0.49	2.57 ± 0.19	1.0	0.91
		K23ac	70.46 ± 9.45	85.1 ± 5.5	1.2	0.23
		K23me3	0.06 ± 0.01	0.1 ± 0.03	1.5	0.40
		K27ac	0.89 ± 0.04	0.76 ± 0.05	0.8	0.08
		K27me1	49.37 ± 2.47	55.36 ± 3.16	1.1	0.19
		K27me2	146.35 ± 2.62	141.34 ± 3.29	1.0	0.28
		K27me3	1.79 ± 0.13	1.82 ± 0.21	1.0	0.88
		K37me2	0.73 ± 0.04	0.61 ± 0.05	0.8	0.08
		K4me1	100 ± 0	100 ± 0	1.0	
		K79me1#	18.71 ± 0.38	19.48 ± 0.21	1.0	0.12
		K79me2#	2.85 ± 0.24	3.25 ± 0.12	1.1	0.20
		R26me2	0.73 ± 0.09	0.51 ± 0.04	0.7	0.07
		R40me1	0.51 ± 0.07	0.42 ± 0.02	0.8	0.23
	H4	R3me1	63.93 ± 2.66	64.88 ± 0.89	1.0	0.75
		R3me2	10.94 ± 1.29	10.13 ± 0.97	0.9	0.64
		K5ac	40.13 ± 3.51	41.2 ± 1.99	1.0	0.80
		K5me1	4.69 ± 1.48	4 ± 0.3	0.9	0.66
		K8ac#	49.64 ± 2.81	48.99 ± 2.13	1.0	0.86
		K8me1	0.5 ± 0.11	0.58 ± 0.12	1.1	0.67
		K12ac#	50.17 ± 5.43	47.72 ± 2.16	1.0	0.69
		R19me1	100 ± 0	100 ± 0	1.0	
		K20me3#	7.58 ± 0.97	5.64 ± 0.5	0.7	0.13
		R23me2	36.62 ± 0.34	36.83 ± 0.32	1.0	0.67

[a]The site, type, and relative abundance of each PTM is indicated. Those which were significantly altered after I/R injury are marked with an asterisk. Those which were verified by WB analysis are marked with #. The intensity of the marks H3K36ac and H3K37me3 were estimated from identified peptides containing the combination H3K36acK37me3. As this combination could not be distinguished by our MS approach from the isobaric form H3K36me3K37ac, the two identifications are considered as ambiguous (marked with §).

The peptides we generated in this study allowed the characterization of several coexisting PTMs on histone H3 and H4, particularly on the most studied combinations H3K9K14, H3K27K36, H4K18K23, H4K5K8K12K16, and H4K20R23. The multiple PTMs detected on histones and their variants are shown in Tables 1 and 2 and Supplemental Tables 1−3 (Supporting Information). Coexisting modifications of histone H3 and H4 were further linked in lines as illustrated in Figure 2. We observed nearby PTMs in combinations, such as acetylation/methylation at K9 and K14, K18 and K23, and K27 and K36 in histone H3 (Figure 2A) and acetylation at K5, K8, K12, and K16 as well as acetylation/methylation at K20 and R23 in histone H4 (Figure 2B).

Table 1 and Figure 3 show the coexisting PTMs on H3, each depicting the detected peptide and its modifications, including the relative abundance of the different peptides identified in the present study. MS analysis of peptides covering residues 9−17 (KSTGGKAPR) revealed a variety of PTMs on H3K9, including acetylation, monomethylation, dimethylation, and trimethylation (Figure 4A and Table 1). H3K9me1 is generally associated with enhancers, and H3K9ac is associated with promoters of actively transcribed genes, while H3K9me2 and H3K9me3 are negatively correlated with gene expression.[30,33]

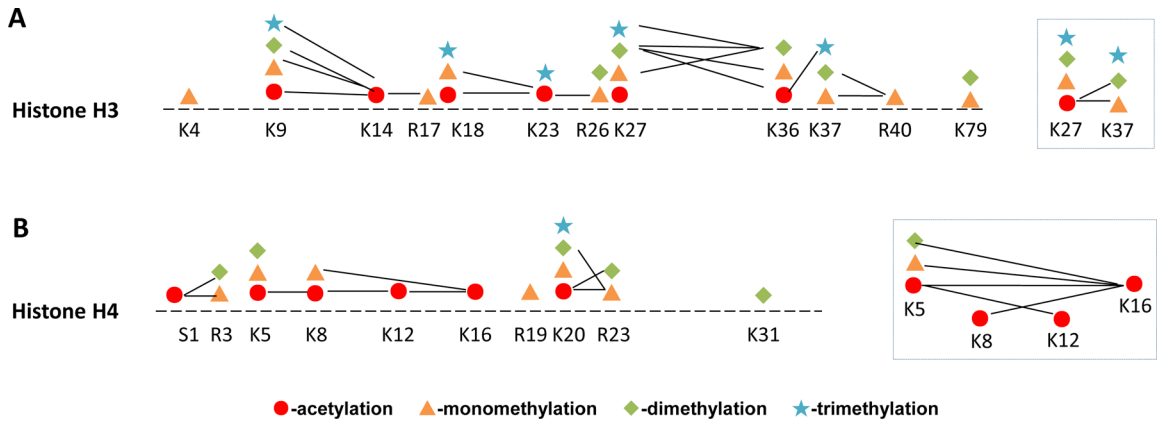

Figure 2. Multiple modification patterns on histone H3 and H4. Coexisting PTMs are illustrated by connecting lines.

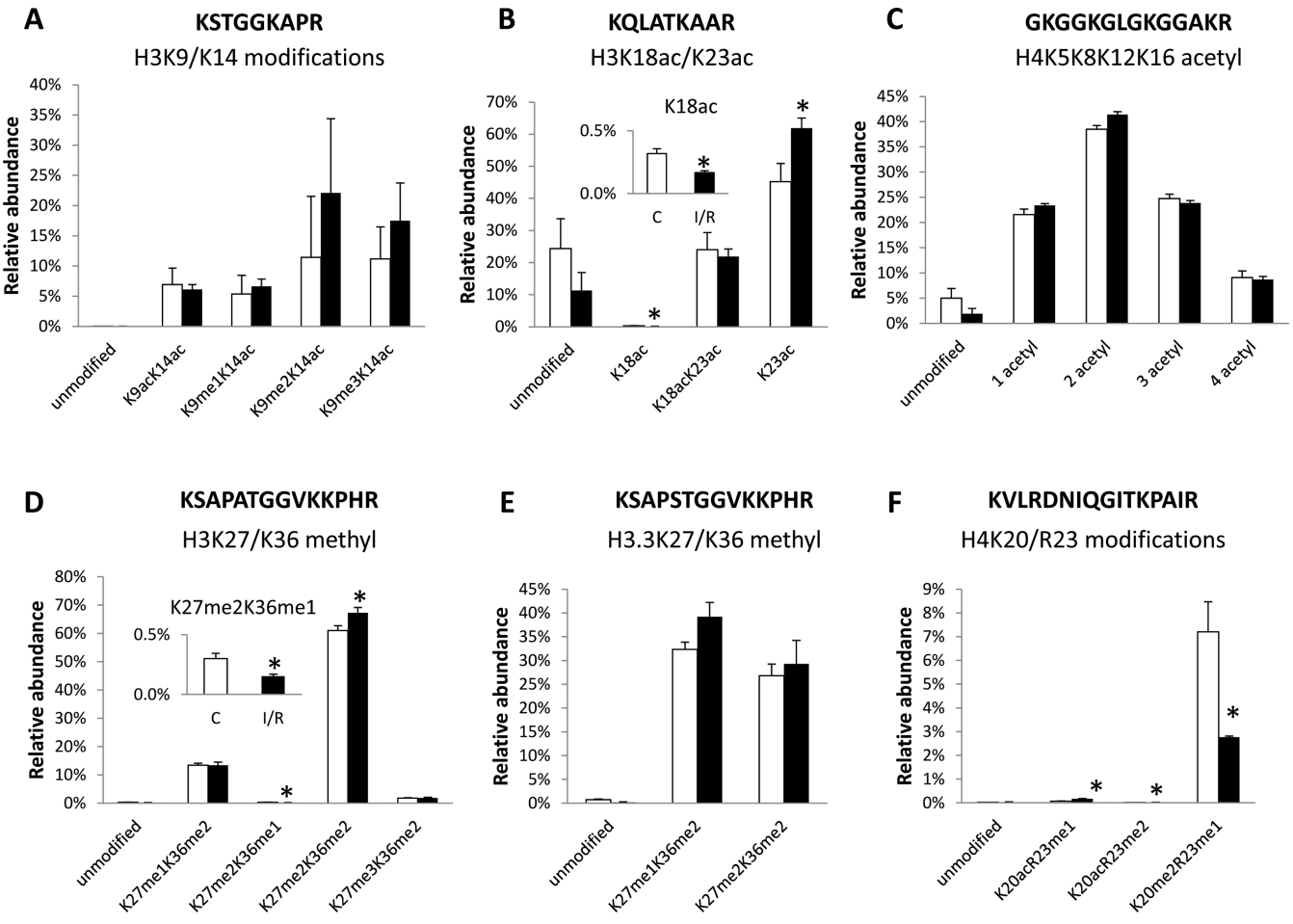

Figure 3. MS analysis of multiple modification patterns in peptides from histone H3 and H4 with and without I/R injury. MS analysis of peptides from histone H3, including (A) H3K9/K14 modifications (aa 9−17), (B) H3K18/K23 acetylation (aa 18−26), (C) K27/K36 methylation from histone H3.1/3.2 (aa 27−40), and (D) from histone H3.3. (E) MS analysis of H4K5K8K12K16 acetylation on the peptide covering GKGGKGLGKGGAKR (aa 4−19) from histone H4 and (F) H4K20/R23 modifications in the peptide covering KVLRDNIQGITKPAIR (aa 20−35). Bar charts represent the relative abundance of the histone modifications. All graphs show the average of four replicates with error bars indicating SEM. Control and I/R injury conditions are colored in white and black, respectively.

Modifications on K9 were not only found isolated but also in combination with H3K14ac (Figure 3A). H3K9ac and H3K14ac have been previously mapped to the promoter region and adjacent to transcription start sites (TSSs) of active genes.[30] In fact, H3K9ac and H3K14ac were also detected as coexisting, suggesting that these two PTMs are not mutually exclusive in rat retina. In noninjured retinas, the coexisting form H3K9acK14ac (frequency: 6.91%) was present in much lower abundance than H3K14ac alone (21.29%) but higher than H3K9ac alone (1.7%) (Table 1). In addition, H3K14ac was also found in combination with monomethylation on H3R17. Furthermore, this specific pattern (H3K14acR17me1) was found significantly less frequently in the retina after I/R injury (control 2.98% vs I/R 1.24%). Acetylation was also observed

dx.doi.org/10.1021/pr500040a | J. Proteome Res. 2014, 13, 2175−2186

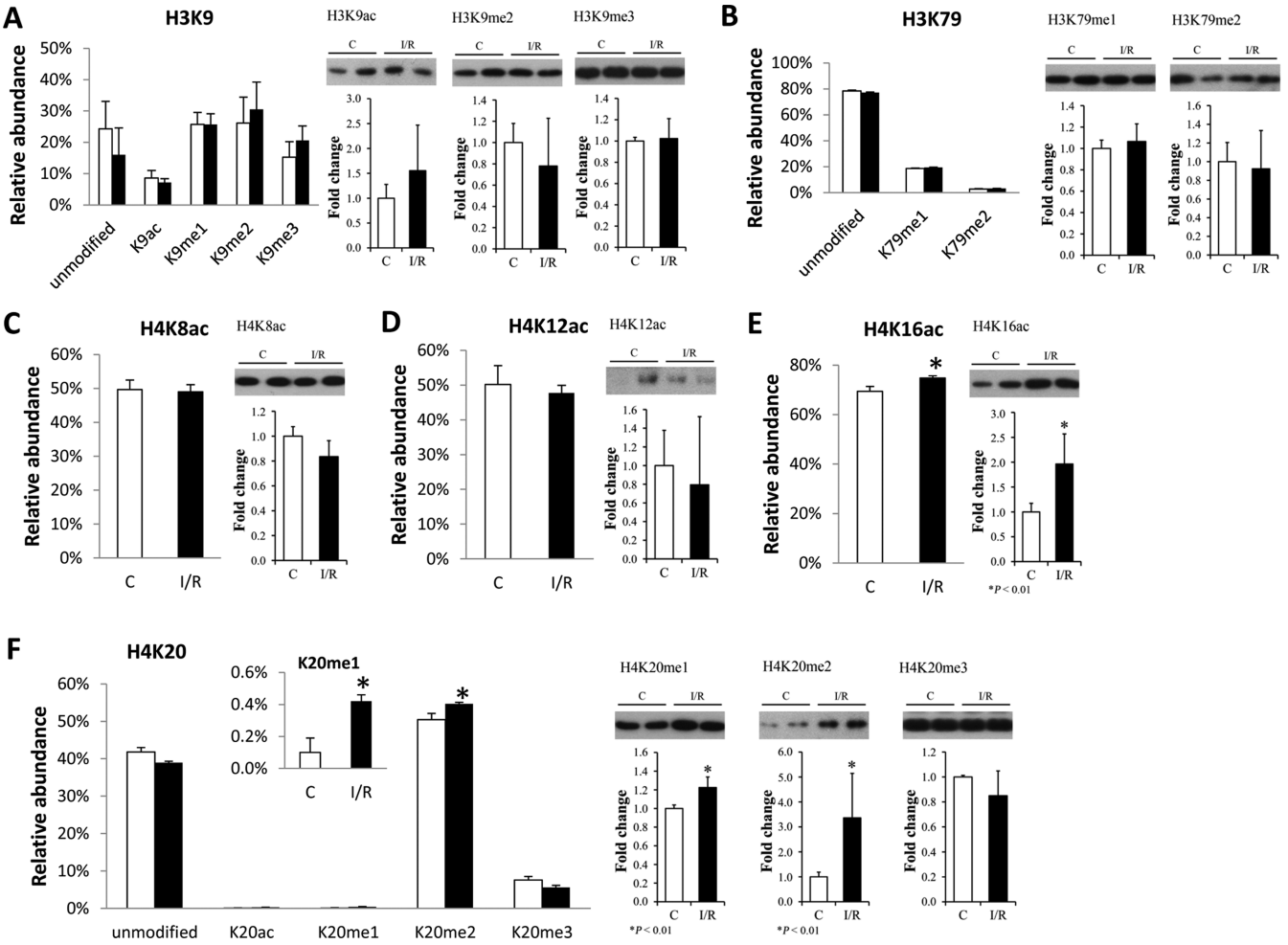

Figure 4. Relative abundance of modifications on (A) H3K9, (B) H3K79, (C) H4K8, (D) H4K12, (E) H3K16, and (F) H4K20 in control and upon I/R injury. Color white represents control while black represents I/R injury. Those which were verified by Western blot are accompanied by Western blot results.

on H3 at residues K18 and K23 through MS analysis of the H3 peptide covering residues 18−26 (KQLATKAAR). Distributions of K18 and K23 in rat retina upon I/R injury are displayed in Supplemental Figure 4A,B (Supporting Information). A variety of PTMs except dimethylation were found on K18. K18 was found largely unmodified with decreasing amounts of K18ac, K18me1, and K18me3. K23 was found to be acetylated and trimethylated in rat retina, whereas other methylated forms were below the detection limit. K23ac was most abundant, followed by unmodified K23 > K23me3. In noninjured retinas, H3K23ac isolated was the most abundant PTM on the given peptide (45.2%), followed by the diacetylated form H3K18acK23ac (24.01%) and H3K18ac isolated (0.32%) (Figure 3B). After I/R injury, H3K18ac isolated showed a decrement, while there was an enrichment in H3K23ac isolated (Figure 3B). H3K23ac was also found coexisting with R26me1 (H3K23acR26me1) in very low abundance (<0.5%) in noninjured retinas; however, this pattern was identified significantly less frequent after I/R injury (Table 1)

MS analysis of the H3 peptide covering residues 27−40 (KSAPATGGVKKPHR) showed a complex pattern of modifications on K27 and K36 in retinas (Table 1 and Figure 3C), consistent with those identified in mammalian cells and other rat tissues.[34,35] These two modifiable sites have a relevant role in gene expression. For instance, H3K27me1 is commonly enriched throughout the body of actively transcribed genes, whereas H3K27me2 and H3K27me3 are enriched on repressed genes.[30,33] H3K36me1 is enriched over active and inactive genes, with H3K36me2 and H3K36me3 enriched throughout the entire transcribed regions of active genes.[30,33,36] Our results demonstrated that in noninjured retinas, the modifications H3K27me2K36me2 in this peptide was the most abundant (61%) (Figure 3C). Interestingly, K27me2 isolated and in combination with methylations at K36 was significantly altered after retinal I/R injury: H3K27me2K36me2 was increased after I/R injury (61.01%/67.24%), while H3K27me2 isolated and K27me2K36me1 were decreased (18.61%/13.81% and 0.3%/0.15%, respectively). In rat, H3.1/3.2 and H3.3 differ by a single amino acid residue at S31 in the first ∼50 amino acids, which is the region considered as the "histone tail" with most of the modifications occur. Therefore, the peptide covering residues 27−40 (KSAPA/STGGVKKPHR) allows for the discrimination of PTMs on K27 and K36 mapped on H3.1/H3.2 and H3.3. It has been demonstrated that H3 variants have distinct PTM patterns in various rat tissues.[37] Consistently, we detected differences in K27 and K36 of H3.1/3.2 and H3.3 in normal retinas (Table 1). The methylated peptides were also the most abundant species present on H3.3 peptide with relatively less complexity compared to H3.1/3.2. However, the relative abundance did not change after I/R injury (Figure 3D). We

dx.doi.org/10.1021/pr500040a | J. Proteome Res. 2014, 13, 2175−2186

also observed the differences in the relative PTM abundance of K27 and K36 between H3.1/3.2 and H3.3. Supplemental Figure 4C (Supporting Information) summarizes the degree of methylation (mono-, di-, and trimethylation) and acetylation on K27 from H3.1/3.2 and H3.3 upon I/R injury. K27me2 predominated followed by K27me1 in both H3.1/3.2 and H3.3. K27me3 was observed in H3.1/3.2 but not in H3.3, whereas K27ac was found in H3.3 but not in H3.1/3.2. As displayed in Supplemental Figure 4D (Supporting Information), K36 was preferentially dimethylated in both H3.1/3.2 and H3.3 in rat retina. Nevertheless, the levels of unmodified K36 and K36me2 varied between H3.1/3.2 and H3.3. K36me2 was the predominant form of H3.1/3.2 (approx.76%) and was 3.5-fold higher than the unmodified form (approx.23%).

Compared to histone H3, histone H4 is more amenable to detailed MS analysis, due to no variant of it. Almost all detectable PTMs are localized in the first 20 aa of histone H4 (Figures 1 and 2). Acetylation was the most common PTM of histone H4 (Table 2). H4 acetylation is known to correlate with gene expression, with H4K5ac, H4K8ac, H4K12ac, and H4K16ac enriched in the promoter and transcribed regions of active genes.[30] The most abundant form of the peptides covering residues 4−17 (GKGGKGLGKGGAKR) of H4 was H4K8acK12ac. Peptides with only one acetylated residue were observed in each of the lysine residues H4K5ac, H4K8ac, H4K12ac, and H4K16ac. The majority of the monoacetylation was observed at position H4K16, consistent with the "zip" model, indicating that histone H4 is modified first at K16 and then PTM occupancy proceeds to K12, K8 and K5.[38] The diacetylated form of this peptide appeared to be most abundant (Figure 3F). A number of diacetylated isomers were identified including H4K5K8, H4K5K16, K8acK12ac, K8acK16ac, and K12acK16ac in the present study (0.95%, 10.71%, 19.71%, 2.86%, and 4.27%, respectively, in noninjured retinas). K5acK16ac increased in abundance after retinal I/R injury (from 10.71% to 12.63%). The mono- and the triacetylated forms of this peptide were similar in abundance (control 21.6%/24.78%, I/R 23.4%/23.88%), whereas the tetra-acetylated form was the least abundant among all the acetylated forms (control 9.11%, I/R 8.7%). The MS analysis of the peptides covering residues 20−35 (KVLRDNIQGITKPAIR) of H4 revealed that methylated species were the most abundant form of this peptide, in particular at sites K20 and R23 (Table 2). Coexisting PTMs on H4K20 and H4R23 were also found to be significantly regulated upon/R injury: K20acR23me1 and K20acR23me2 appeared to increase by more than 2-fold after injury, whereas K20me2R23me1 showed the opposite trend (Figure 3F).

In addition to H3 and H4, we also characterized the other histone proteins H2A, H2B, and H1 and their variants upon retinal I/R injury. As indicated in Supplemental Tables 1−3 (Supporting Information), a broad spectrum of PTMs was quantified. A total of nine modifications including coexisting ones were also found to be affected by I/R injury. A number of histone variants are not included in the rat database, but we found some peptides matching in the MS results. This would suggest that these variants exist also in rat and not only in mouse, which is more deeply characterized.

Rat Retinal Histone PTMs and Validations of I/R Injury-Induced Changes by Western Blotting Analysis

The quantitative information of individual histone PTMs identified in the present study are included in Table 3. We selected 11 different commercial antibodies for Western blot (WB) confirmation of the MS results. The choice was based on antibody availability and interest in the specific PTM. The distribution of K9 modifications is displayed in Figure 4A. In the noninjured rat retina, K9me2 and K9me1 were the most abundant modifications found in a nearly 1:1 ratio followed by K9me3 > unmodified K9 > K9ac. No significant changes were observed for the single marks, and this was confirmed by WB observations. We also verified the levels of mono- and dimethylation of K79, a mark associated with actively transcribed genes.[30,33] The unmodified peptide was the most abundant form present in noninjured retina (78.44%), followed by H3K79me1 (18.71%) and H3K79me2 (2.85%), with no significant changes observed after the injury (Figure 4B). No significant change in total histone H3 level was found between the I/R injured group and the noninjured group by WB analysis (Supplemental Figure 5, Supporting Information).

In histone H4, the most abundant modifications were acetylations on K5/K8/K12/K16 and K20me2 (Table 3, Figure 4C−F, and Supplemental Figure 4E (Supporting Information)). H4K16ac significantly increased after I/R injury (69.43%/74.74%, Figure 4E). The extensively studied site H4K20 has been detected with all different modifications (Figure 4F). The most abundant form was H4K20me2 (50.44%) in noninjured retina. This PTM, together with H4K20me1 were all significantly increased after retinal I/R injury (50.44%/54.66%, 0.1%/0.42%). All these changes could be confirmed by WBs. Other poorly annotated H4 PTMs showed significant changes between the two conditions such as H4R23me1, which was found less frequent after treatment (12.42%/5.05%) (Supplemental Figure 4F, Supporting Information). However, we could not retrieve a specific antibody for confirmation. Again, no significant change in total histone H4 level was found between I/R injured group and noninjured group by WB analysis (Supplemental Figure 5, Supporting Information).

In summary, 34 histone PTMs (corresponding to 26% of all the identified ones) showed significant increased or decreased abundance after I/R injury. In particular, we observed significant changes for seven PTMs on H3, six on H4, 13 on H2A, one on H2B, and seven on H1 (Table 3 and Supplemental Table 3, Supporting Information). We applied Western blotting to confirm the reliability of the results obtained by the LC−MS/MS analysis by using commercially available antibodies, in particular, for histone H3 and H4. We verified the abundance of H3K9ac, H3K9me2, H3K9me3, H3K79me1, H3K79me2 and H4K8ac, H4K12ac, H4K20me1, H4K20me2, and H4K20me3. Results appeared to be consistent with our findings (Figure 4).

DNA Damage upon I/R Injury

Interestingly, we observed a specific and significant increase of the methylation of H4K20 for K20me2 and K20me1 (Figure 4F). Increased abundance of the histone mark H4K20me2 is associated with DNA damage.[21−23] Therefore, we further investigated the DNA damage signaling pathway after I/R injury. DNA damage triggers DNA repair and results in accumulation of phosphorylated p53[39,40] and phosphorylated Chk1[41] to participate in DNA repair. γ-H2AX is also a marker of DNA damage.[42,43] As shown in Figure 5, significant up-regulation of γ-H2AX, total p53, p-p53(phosphorylated p53), and p-Chk1(phosphorylated Chk1) were found in the injured retinas, suggesting severe DNA damage following I/R injury.

dx.doi.org/10.1021/pr500040a | J. Proteome Res. 2014, 13, 2175−2186

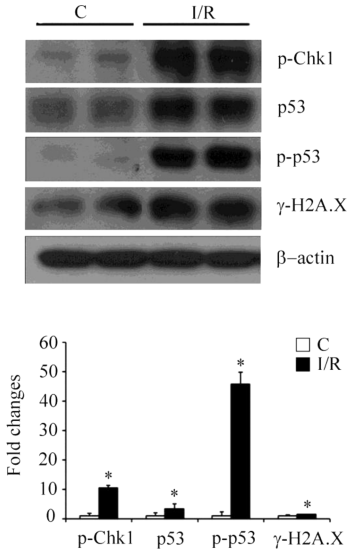

Figure 5. DNA damage in I/R retina. Up panel, representative Western blots of p-Chk1, p53, p-p53, γ-H2AX, and β-actin. Bottom panel, densitometric quantitative results of p-Chk1, p53, p-p53, and γ-H2AX levels after retinal I/R injury: C, noninjured eyes; I/R, retinal I/R-injured eye. (n = 6, each group; *p < 0.05 compared with noninjured group).

CONCLUSION

In this work, we determined and compared PTM patterns of rat retinal histone proteins upon I/R injury. We employed both LC−-MS/MS and Western blotting analysis. Our results showed that retinal histones are extensively modified by PTMs, including mono-, di-, and trimethylation and acetylation and combinations of these modifications within same histone protein. Our study provides the most comprehensive characterization of PTM patterns of rat retinal histones to date. A number of histone PTM patterns were significantly altered upon I/R injury concomitant with activation of the DNA damage response. Further functional studies are required to investigate the biological significance of these coexisting PTMs, which could provide new insights into the regulation of gene expression and chromatin structure in the pathogenesis of ocular diseases.

ASSOCIATED CONTENT

Supporting Information

Supplemental Figure 1: Extracted retinal histone separated by TAU-SDS-PAGE and AU-SDS-PAGE and MS identifications of the gel spots. A combination of 2D-gel separation and in-gel propionylation/trypsin digestion followed by LC−MS−MS analysis was used to identify histone proteins. Extracted histones from I/R-injured and noninjured retinas were separated by either TAU-SDS PAGE or AU-SDS PAGE. I/R-induced histones changed in spot size and tailing in at least five different places, indicating alteration of certain histone variants and histone PTMs. Marked regions corresponding to the five differences between control (C) and I/R. Extracted histones were first chemically derivatized using propionic anhydride and were subsequently digested using trypsin. The generated peptides were further analyzed using online LC-MS/MS performed on an Eksigent Tempo nano MDLC system coupled with a QSTAR Elite mass spectrometer (AB Sciex). Supplemental Figure 2: Correlation between replicate analyses. In the box, R^2 correlation values of the relative abundance of histone marks between replicates and between samples. C and I/R indicate control and ischemia samples, respectively. On the top right in green, correlation values for the relative abundance of single marks. On the bottom left in yellow, same for the coexisting marks. Correlation values for coexisting marks are generally lower than single ones. However, the average R^2 was 0.92, indicating a good correlation between replicates and samples. Supplemental Figure 3: Dynamic range between quantified histone marks. LC−MS extracted chromatogram of the peptide KVLRDNIQGITKPAIR modified as H4K20acR23me1 (above) and H4K20me2 (below) in one of the control replicates. The figure displays the protein occupancy for the given PTMs estimated in the current analysis. The peak area integration for the specific PTM patterns shows the wide dynamic range between the abundant marks we identified (∼50% of the total protein) and the low abundant ones (<0.1%). Supplemental Figure 4: Relative abundance of modifications on (A) H3K18 (B) H3K23 (C) H3K27 (D) H3K36 (E) H4K5 (F) H4R23 in control (white) and upon I/R injury (black). Supplemental Figure 5: Total histone H3 and H4 levels after retinal I/R injury. On the left panel, representative Western blots of total histone H3 and H4 and corresponding Coomassie blue staining. On the right panel, densitometric quantitative results of total histone H3 and H4 levels after retinal I/R injury. Supplemental Table 1: Quantified H2A peptides. Those which were significantly altered after I/R injury are marked with an asterisk. Supplemental Table 2: Quantified H2B peptides. Those which were significantly altered after I/R injury are marked with an asterisk. Supplemental Table 3: Quantified H1 peptides. Those which were significantly altered after I/R injury are marked with *. Supplemental Table 4: Relative abundances of single histone marks. Supplemental Table 5: Relative abundances of coexisting histone marks. Supplemental Table 6: Information of all identified peptides by LC−MS/MS. This material is available free of charge via the Internet at http://pubs.acs.org.

AUTHOR INFORMATION

Corresponding Authors

*E-mail: lzheng@whu.edu.cn. Tel: + 86-27-68755559. Fax: + 86-27-68755559.
*E-mail: jenseno@bmb.sdu.dk. Tel: +45 6550 2368. Fax: +45 6550 2467.
*E-mail: guol@whu.edu.cn. Tel: + 86-27-68753800. Fax + 86-27-68753797.

Notes

The authors declare no competing financial interest.

ACKNOWLEDGMENTS

This work was supported by the National Basic Research Program of China (2012CB524901), the Natural Science Foundation of China (Nos. 81100687 and 31271370), the Doctoral Foundation of Ministry of Education of China, 2011, the China Postdoctoral Science Foundation Grant (2012M511660), and the Natural Science Foundation of Hubei Province (X.Z., 2012). Work in the ONJ laboratory was financed by a generous grant from the Danish National Research Foundation to the Center for Epigenetics (Grant No. DNRF82).

ABBREVIATIONS

I/R, ischemia and reperfusion
TCA, trichloroacetic acid
LC, liquid chromatography
LTQ, 2D linear ion trap
MS, mass spectrometry
MS/MS, tandem mass spectrometry
MSA, multistage activation
PTM, post-translational modification
RP, reversed phase
CID, collision-induced dissociation

REFERENCES

(1) Szabo, M. E.; Haines, D.; Garay, E.; Chiavaroli, C.; Farine, J. C.; Hannaert, P.; Berta, A.; Garay, R. P. Antioxidant properties of calcium dobesilate in ischemic/reperfused diabetic rat retina. *Eur. J. Pharmacol.* **2001**, *428* (2), 277−86.

(2) Kawai, S. I.; Vora, S.; Das, S.; Gachie, E.; Becker, B.; Neufeld, A. H. Modeling of risk factors for the degeneration of retinal ganglion cells after ischemia/reperfusion in rats: effects of age, caloric restriction, diabetes, pigmentation, and glaucoma. *FASEB J.* **2001**, *15* (7), 1285−7.

(3) Zheng, L.; Gong, B.; Hatala, D. A.; Kern, T. S. Retinal ischemia and reperfusion causes capillary degeneration: similarities to diabetes. *Invest. Ophthalmol. Vis. Sci.* **2007**, *48* (1), 361−7.

(4) Wang, L.; Li, C.; Guo, H.; Kern, T. S.; Huang, K.; Zheng, L. Curcumin inhibits neuronal and vascular degeneration in retina after ischemia and reperfusion injury. *PLoS One* **2011**, *6* (8), e23194.

(5) Osborne, N. N.; Casson, R. J.; Wood, J. P.; Chidlow, G.; Graham, M.; Melena, J. Retinal ischemia: mechanisms of damage and potential therapeutic strategies. *Prog. Retin Eye Res* **2004**, *23* (1), 91−147.

(6) Baumeister, P.; Dong, D.; Fu, Y.; Lee, A. S. Transcriptional induction of GRP78/BiP by histone deacetylase inhibitors and resistance to histone deacetylase inhibitor-induced apoptosis. *Mol. Cancer Ther.* **2009**, *8* (5), 1086−94.

(7) Zheng, L.; Liu, S.; Sun, M. Z.; Chang, J.; Chance, M. R.; Kern, T. S. Pharmacologic intervention targeting glycolytic-related pathways protects against retinal injury due to ischemia and reperfusion. *Proteomics* **2009**, *9* (7), 1869−82.

(8) Galasinski, S. C.; Louie, D. F.; Gloor, K. K.; Resing, K. A.; Ahn, N. G. Global regulation of post-translational modifications on core histones. *J. Biol. Chem.* **2002**, *277* (4), 2579−88.

(9) Zhao, L.; Wang, P.; Yan, S.; Gao, F.; Li, H.; Hou, H.; Zhang, Q.; Tan, J.; Li, L. Promoter-associated histone acetylation is involved in the osmotic stress-induced transcriptional regulation of the maize ZmDREB2A gene. *Physiol Plant* **2013**.

(10) Evertts, A. G.; Manning, A. L.; Wang, X.; Dyson, N. J.; Garcia, B. A.; Coller, H. A. H4K20 methylation regulates quiescence and chromatin compaction. *Mol. Biol. Cell* **2013**, *24* (19), 3025−37.

(11) Huang, S. K.; Scruggs, A. M.; Donaghy, J.; Horowitz, J. C.; Zaslona, Z.; Przybranowski, S.; White, E. S.; Peters-Golden, M. Histone modifications are responsible for decreased Fas expression and apoptosis resistance in fibrotic lung fibroblasts. *Cell Death Dis.* **2013**, *4*, e621.

(12) Wolf, L.; Harrison, W.; Huang, J.; Xie, Q.; Xiao, N.; Sun, J.; Kong, L.; Lachke, S. A.; Kuracha, M. R.; Govindarajan, V.; Brindle, P. K.; Ashery-Padan, R.; Beebe, D. C.; Overbeek, P. A.; Cvekl, A. Histone posttranslational modifications and cell fate determination: lens induction requires the lysine acetyltransferases CBP and p300. *Nucleic Acids Res.* **2013**, *41* (22), 10199−214.

(13) Sundar, I. K.; Nevid, M. Z.; Friedman, A. E.; Rahman, I. Cigarette Smoke Induces Distinct Histone Modifications in Lung Cells: Implications for the Pathogenesis of COPD and Lung Cancer. *J. Proteome Res.* **2013**.

(14) Lee, J.; Hwang, Y. J.; Shin, J. Y.; Lee, W. C.; Wie, J.; Kim, K. Y.; Lee, M. Y.; Hwang, D.; Ratan, R. R.; Pae, A. N.; Kowall, N. W.; So, I.; Kim, J. I.; Ryu, H. Epigenetic regulation of cholinergic receptor M1 (CHRM1) by histone H3K9me3 impairs Ca(2+) signaling in Huntington's disease. *Acta Neuropathol* **2013**, *125* (5), 727−39.

(15) Xia, M.; Liu, J.; Wu, X.; Liu, S.; Li, G.; Han, C.; Song, L.; Li, Z.; Wang, Q.; Wang, J.; Xu, T.; Cao, X. Histone methyltransferase Ash1l suppresses interleukin-6 production and inflammatory autoimmune diseases by inducing the ubiquitin-editing enzyme A20. *Immunity* **2013**, *39* (3), 470−81.

(16) Popova, E. Y.; Xu, X.; DeWan, A. T.; Salzberg, A. C.; Berg, A.; Hoh, J.; Zhang, S. S.; Barnstable, C. J. Stage and gene specific signatures defined by histones H3K4me2 and H3K27me3 accompany mammalian retina maturation in vivo. *PLoS One* **2012**, *7* (10), e46867.

(17) Zhong, Q.; Kowluru, R. A. Regulation of matrix metalloproteinase-9 by epigenetic modifications and the development of diabetic retinopathy. *Diabetes* **2013**, *62* (7), 2559−68.

(18) Kadiyala, C. S.; Zheng, L.; Du, Y.; Yohannes, E.; Kao, H. Y.; Miyagi, M.; Kern, T. S. Acetylation of retinal histones in diabetes increases inflammatory proteins: effects of minocycline and manipulation of histone acetyltransferase (HAT) and histone deacetylase (HDAC). *J. Biol. Chem.* **2012**, *287* (31), 25869−80.

(19) Wang, L. L.; Chen, H.; Huang, K.; Zheng, L. Elevated histone acetylations in Muller cells contribute to inflammation: a novel inhibitory effect of minocycline. *Glia* **2012**, *60* (12), 1896−905.

(20) Sidoli, S.; Cheng, L.; Jensen, O. N. Proteomics in chromatin biology and epigenetics: Elucidation of post-translational modifications of histone proteins by mass spectrometry. *J. Proteomics* **2012**, *75* (12), 3419−33.

(21) Hsiao, K. Y.; Mizzen, C. A. Histone H4 deacetylation facilitates 53BP1 DNA damage signaling and double-strand break repair. *J. Mol. Cell Biol.* **2013**, *5* (3), 157−65.

(22) Pei, H.; Zhang, L.; Luo, K.; Qin, Y.; Chesi, M.; Fei, F.; Bergsagel, P. L.; Wang, L.; You, Z.; Lou, Z. MMSET regulates histone H4K20 methylation and 53BP1 accumulation at DNA damage sites. *Nature* **2011**, *470* (7332), 124−8.

(23) Sanders, S. L.; Arida, A. R.; Phan, F. P. Requirement for the phospho-H2AX binding module of Crb2 in double-strand break targeting and checkpoint activation. *Mol. Cell. Biol.* **2010**, *30* (19), 4722−31.

(24) Chung, S.; Sundar, I. K.; Hwang, J. W.; Yull, F. E.; Blackwell, T. S.; Kinnula, V. L.; Bulger, M.; Yao, H.; Rahman, I. NF-kappaB inducing kinase, NIK mediates cigarette smoke/TNFalpha-induced histone acetylation and inflammation through differential activation of IKKs. *PLoS One* **2011**, *6* (8), e23488.

(25) Shechter, D.; Dormann, H. L.; Allis, C. D.; Hake, S. B. Extraction, purification and analysis of histones. *Nat. Protoc.* **2007**, *2* (6), 1445−57.

(26) Kim, I. S.; Lee, M.; Park, K. C.; Jeon, Y.; Park, J. H.; Hwang, E. J.; Jeon, T. I.; Ko, S.; Lee, H.; Baek, S. H.; Kim, K. I. Roles of Mis18alpha in epigenetic regulation of centromeric chromatin and CENP-A loading. *Mol. Cell* **2012**, *46* (3), 260−73.

(27) Pesavento, J. J.; Mizzen, C. A.; Kelleher, N. L. Quantitative analysis of modified proteins and their positional isomers by tandem mass spectrometry: human histone H4. *Anal. Chem.* **2006**, *78* (13), 4271−80.

(28) Latham, J. A.; Dent, S. Y. Cross-regulation of histone modifications. *Nat. Struct. Mol. Biol.* **2007**, *14* (11), 1017−24.

(29) Fischle, W.; Wang, Y.; Allis, C. D. Histone and chromatin cross-talk. *Curr. Opin. Cell Biol.* **2003**, *15* (2), 172−83.

(30) Wang, Z.; Zang, C.; Rosenfeld, J. A.; Schones, D. E.; Barski, A.; Cuddapah, S.; Cui, K.; Roh, T. Y.; Peng, W.; Zhang, M. Q.; Zhao, K. Combinatorial patterns of histone acetylations and methylations in the human genome. *Nat. Genet.* **2008**, *40* (7), 897−903.

(31) Bannister, A. J.; Kouzarides, T. Regulation of chromatin by histone modifications. *Cell Res.* **2011**, *21* (3), 381−95.

(32) Yuan, W.; Xu, M.; Huang, C.; Liu, N.; Chen, S.; Zhu, B. H3K36 methylation antagonizes PRC2-mediated H3K27 methylation. *J. Biol. Chem.* **2011**, *286* (10), 7983−9.

(33) Barski, A.; Cuddapah, S.; Cui, K.; Roh, T. Y.; Schones, D. E.; Wang, Z.; Wei, G.; Chepelev, I.; Zhao, K. High-resolution profiling of

histone methylations in the human genome. *Cell* **2007**, *129* (4), 823–37.
(34) Garcia, B. A.; Mollah, S.; Ueberheide, B. M.; Busby, S. A.; Muratore, T. L.; Shabanowitz, J.; Hunt, D. F. Chemical derivatization of histones for facilitated analysis by mass spectrometry. *Nat. Protoc.* **2007**, *2* (4), 933–8.
(35) Tweedie-Cullen, R. Y.; Brunner, A. M.; Grossmann, J.; Mohanna, S.; Sichau, D.; Nanni, P.; Panse, C.; Mansuy, I. M. Identification of combinatorial patterns of post-translational modifications on individual histones in the mouse brain. *PLoS One* **2012**, *7* (5), e36980.
(36) Bannister, A. J.; Schneider, R.; Myers, F. A.; Thorne, A. W.; Crane-Robinson, C.; Kouzarides, T. Spatial distribution of di- and trimethyl lysine 36 of histone H3 at active genes. *J. Biol. Chem.* **2005**, *280* (18), 17732–6.
(37) Garcia, B. A.; Thomas, C. E.; Kelleher, N. L.; Mizzen, C. A. Tissue-specific expression and post-translational modification of histone H3 variants. *J. Proteome Res.* **2008**, *7* (10), 4225–36.
(38) Zhang, K.; Williams, K. E.; Huang, L.; Yau, P.; Siino, J. S.; Bradbury, E. M.; Jones, P. R.; Minch, M. J.; Burlingame, A. L. Histone acetylation and deacetylation: identification of acetylation and methylation sites of HeLa histone H4 by mass spectrometry. *Mol. Cell Proteomics* **2002**, *1* (7), 500–8.
(39) Huang, Y. C.; Hung, W. C.; Kang, W. Y.; Chen, W. T.; Chai, C. Y. p-Phenylenediamine induced DNA damage in SV-40 immortalized human uroepithelial cells and expression of mutant p53 and COX-2 proteins. *Toxicol. Lett.* **2007**, *170* (2), 116–23.
(40) Heo, J. I.; Oh, S. J.; Kho, Y. J.; Kim, J. H.; Kang, H. J.; Park, S. H.; Kim, H. S.; Shin, J. Y.; Kim, M. J.; Kim, M.; Kim, S. C.; Park, J. B.; Kim, J.; Lee, J. Y. ATM mediates interdependent activation of p53 and ERK through formation of a ternary complex with p-p53 and p-ERK in response to DNA damage. *Mol. Biol. Rep.* **2012**, *39* (8), 8007–14.
(41) Yarden, R. I.; Metsuyanim, S.; Pickholtz, I.; Shabbeer, S.; Tellio, H.; Papa, M. Z. BRCA1-dependent Chk1 phosphorylation triggers partial chromatin disassociation of phosphorylated Chk1 and facilitates S-phase cell cycle arrest. *Int. J. Biochem. Cell Biol.* **2012**, *44* (11), 1761–9.
(42) Tanaka, T.; Halicka, D.; Traganos, F.; Darzynkiewicz, Z. Cytometric analysis of DNA damage: phosphorylation of histone H2AX as a marker of DNA double-strand breaks (DSBs). *Methods Mol. Biol.* **2009**, *523*, 161–8.
(43) Sharma, A.; Singh, K.; Almasan, A. Histone H2AX phosphorylation: a marker for DNA damage. *Methods Mol. Biol.* **2012**, *920*, 613–26.